The Photosystem of *Rhodobacter sphaeroides* Assembles with Zinc Bacteriochlorophyll in a *bchD* (Magnesium Chelatase) Mutant†

Paul R. Jaschke and J. Thomas Beatty*

Department of Microbiology and Immunology, The University of British Columbia, 2350 Health Sciences Mall, Vancouver, British Columbia, Canada V6T 1Z3

Received July 17, 2007; Revised Manuscript Received August 20, 2007

ABSTRACT: A *Rhodobacter sphaeroides bchD* (magnesium chelatase) mutant was studied to determine the properties of its photosystem in the absence of bacteriochlorophyll (BChl). Western blots of reaction center H, M, and L (RC H/M/L) proteins from mutant membranes showed levels of 12% RC H, 32% RC L, and 46% RC M relative to those of the wild type. Tricine−SDS−PAGE revealed 52% light-harvesting complex α chain and 14% *β* chain proteins compared to those of the wild type. Pigment analysis of *bchD* cells showed the absence of BChl and bacteriopheophytin (BPhe), but zinc bacteriochlorophyll (Zn-BChl) was discovered. Zn-BChl binds to light-harvesting 1 (LH1) and 2 (LH2) complexes in place of BChl in *bchD* membranes, with a LH2:LH1 ratio resembling that of wild-type cells under BChl-limiting conditions. Furthermore, the RC from the *bchD* mutant contained Zn-BChl in the special pair and accessory BChl binding sites, as well as carotenoid and quinone, but BPhe was absent. Comparison of the *bchD* mutant RC absorption spectrum to that of *Acidiphilium rubrum*, which contains Zn-BChl in the RC, suggests the RC protein environment at L168 contributes to *A. rubrum* special pair absorption characteristics rather than solely Zn-BChl. We speculate that Zn-BChl is synthesized via the normal BChl biosynthetic pathway, but with ferrochelatase supplying zinc protoporphyrin IX for enzymatic steps following the nonfunctional magnesium chelatase. The absence of BPhe in *bchD* cells is likely related to Zn^{2+} stability in the chlorin macrocycle and consequently high resistance of Zn-BChl to pheophytinization (dechelation). Possible agents prevented from dechelating Zn-BChl include the RC itself, a hypothetical dechelatase enzyme, and spontaneous processes.

The presence of membrane-bound light-harvesting and reaction center complexes (the photosystem) in the photosynthetic purple non-sulfur bacterium *Rhodobacter sphaeroides* is repressed by high concentrations of O_2 and induced in response to low concentrations of O_2 (*1*). Photosystem assembly has been studied by shifting cultures from high to low O_2 growth conditions to reveal the regulation of many genes involved in pigment biosynthesis and production of photosystem proteins (*1*). During such shifts the cytoplasmic membrane is thought to expand at specific regions to create invaginations which mature into an intracytoplasmic membrane system (ICM)[1] contiguous with the cytoplasmic membrane (*2*). The photosystem is housed in the ICM (*2*) and uses light energy to drive electron-transfer reactions that result in the net transport of protons from the cytoplasm to the periplasm, which generates a transmembrane electrochemical gradient that is used primarily for ATP synthesis (*3*).

The core of the purple bacterial photosystem is a dimer of reaction center (RC) complexes surrounded by the light-harvesting complex 1 (LH1) and the PufX protein (*4*−*6*). In the ICM, RC/LH1/PufX dimers appear to form linear arrays surrounded by a pool of light-harvesting complex 2 (LH2) (*7*). LH1 and LH2 are rings of α and *β* proteins that bind carotenoid and bacteriochlorophyll (BChl) pigments which absorb and transmit light energy to the RC complex. The RC contains three proteins called H, M, and L (*8*), with the structurally similar RC M and L proteins consisting of five transmembrane helices with pseudo-2-fold symmetry, whereas the RC H protein has only one transmembrane helix and a large cytoplasmic domain (*9*). Embedded within the protein scaffold of the RC are 10 cofactors, some of which participate directly in light-driven electron and proton transfers. The "special pair" BChl dimer (also known as D or P) is bound by RC M and L on the periplasmic side of the membrane. The special pair is flanked by two accessory (or "voyeur") monomeric BChls bound to RC L (B_A) and RC M (B_B), which are the periplasmic ends of two branches of cofactors in the RC structure. The two branches are called A and B, and only the A branch pigments function in electron transfer.

† This research was supported by UBC UGF (Grant 6302) and NSERC PGS-M (Grant 317942) scholarships to P.R.J. and an NSERC Discovery grant to J.T.B.

* To whom correspondence should be addressed. Phone: (604) 822-6896. Fax: (604) 822-6041. E-mail: jbeatty@interchange.ubc.ca.

[1] Abbreviations: 6His, six-histidine tag; ALA, 5-aminolevulinic acid; $B_{A,B}$, accessory bacteriochlorophyll binding sites of the reaction center; BChl, bacteriochlorophyll *a*; (B)Chl, (bacterio)chlorophyll; BPhe, bacteriopheophytin; DCTB, *trans*-2-[3-(4-*tert*-butylphenyl)-2-methyl-2-propenylidene]malononitrile; $H_{A,B}$, bacteriopheophytin binding sites of the reaction center; ICM, intracytoplasmic membrane; LDAO, lauryldimethylamine *N*-oxide; LH, light-harvesting; LH1, light-harvesting complex 1; LH2, light-harvesting complex 2; *m*/*z*, mass to charge ratio; PPIX, protoporphyrin IX; $Q_{A,B}$, quinone binding sites of the reaction center; RC, reaction center; RC H, reaction center H protein; RC M, reaction center M protein; RC L, reaction center L protein; Zn-BChl, zinc bacteriochlorophyll *a*; Zn-PPIX, zinc protoporphyrin IX.

10.1021/bi701407k CCC: $37.00
Published on Web 10/02/2007

Two bacteriopheophytin (BPhe) molecules (H_A and H_B) are located between the accessory BChls and two quinones (Q_A and Q_B) which are bound near the cytoplasmic side of the RC. An iron (Fe^{2+}) atom is located between Q_A and Q_B, and a carotenoid is bound near the B branch accessory BChl (*9*). After absorption of a photon of light by the special pair an electron is transferred through the A branch and then to the Q_B quinone. After two electron and two proton transfers to Q_B, the resultant Q_BH_2 leaves the RC and is oxidized in the cytochrome b/c_1 complex (*3*).

The biosynthesis of tetrapyrroles begins with 5-aminolevulinic acid (ALA), which is converted through several enzymatic steps to protoporphyrin IX (PPIX), a precursor of heme and BChl (*10*). The first committed step of BChl synthesis is the insertion of Mg^{2+} into the macrocycle of PPIX in an ATP-dependent manner by the magnesium chelatase enzyme. This enzyme is encoded by the *bchIHD* genes and has been shown to require all three subunits for enzyme activity (*11*). Multiple enzymatic reactions convert Mg-PPIX to BChl, with the later steps thought to take place in the ICM, perhaps for BChl delivery to nascent RC and LH complexes (*12*).

The relationship among photosystem proteins, membranes, and pigments has been studied extensively in bacteria and plants. Early work on *Rba. sphaeroides* mutants that are incapable of BChl biosynthesis showed incomplete ICM maturation (*13*), which is similar to the phenotype seen in chloroplast membranes of rice plants with a disruption of the gene homologous to *bchD* (*14*). Photosystem proteins seem to be stabilized by the presence of pigments in plants (*15*, *16*) and bacteria (*17*). Pulse-chase experiments on a *bchH* mutant of *Rhodobacter capsulatus* showed that RC and LH proteins were synthesized and membrane-inserted, but the LH proteins were much less stable than in a wild-type strain (*18*). Similarly, it was recently shown that, in *bchI* homologue knock-down tobacco plants, light-harvesting proteins were present in the chloroplast membrane at drastically reduced levels (*19*). Experiments on *Rba. sphaeroides* mutants that uncharacteristically produce BChl under aerobic growth conditions indicated that the main stabilizing influence on the RC proteins is the presence of BChl, and not other factors relating to low O_2 levels during growth (*17*, *20*). The structural role of BChl and BPhe in the *Rba. sphaeroides* RC has been explored using single amino acid changes in the RC M and L proteins that cause BChl instead of BPhe to bind to the H_A and H_B sites or exclusion of BPhe from the H_B site. Despite these changes, the mutant RCs are capable of assembling and supporting photosynthetic growth (*21*, *22*).

In this paper we describe experiments on a magnesium chelatase subunit D (*bchD*) mutant of *Rba. sphaeroides* to quantitatively measure the effects of the *bchD* mutation on the cellular amounts of LH and RC proteins, as well as photosynthetic pigments and complexes. It was found that the *bchD* mutant produces significantly lower amounts of LH and RC proteins compared to the parental (wild-type) strain, but that these proteins form complexes with a BChl-like pigment. We confirmed that the *bchD* mutant does not synthesize BChl (*23*) and discovered the presence of a pigment with a mass that differs from that of BChl by the substitution of Zn^{2+} in place of Mg^{2+} in the chlorin macrocycle (Zn-BChl). The novel RC complex produced in this mutant was purified, and the absorption spectrum and pigment composition were determined. The results indicate the presence of Zn-BChl in the special pair and accessory BChl sites, but the absence of BPhe in the H_A and H_B sites. Thus, this work shows that *Rba. sphaeroides* synthesizes Zn-BChl in the absence of a functional magnesium chelatase and assembles LH and RC complexes containing Zn-BChl in the complete absence of BPhe.

MATERIALS AND METHODS

Bacterial Strains, Plasmids, Growth of Cultures, and Membrane Isolation. The wild-type *Rba. sphaeroides* strain NCIB8253 and the *bchD* mutant TB59 created in the NCIB8253 background by transposon Tn5 insertion into the *bchD* gene (restriction mapped to the 3′-end of the gene) (*23*) were grown as described previously (*24*), using LB medium (pH 7, and which normally contains approximately 12.8 μM Zn^{2+} (*25*)). High to low aeration shifted cultures were initially grown in flasks filled to 20% volume, rotated at 300 rpm until the early exponential phase, and then used to seed a flask filled to 80% volume and rotated at 150 rpm. Cells were harvested 8 h after the shift.

The plasmid p6His-C contains the gene *puhA* encoding the RC H protein fused at the C-terminus to six histidine codons, under control of the *puc* operon promoter (*26*). The otherwise isogenic plasmid pATP19P (*27*) lacks a *puhA* gene insert. These plasmids were introduced into *Rba. sphaeroides* strains NCIB8253 and TB59 by conjugation using *Escherichia coli* strain S17-1 as the donor (*28*).

Cells were disrupted in a French press and membranes isolated by ultracentrifugation as described previously (*24*).

His-Tag Pull-Downs. For analysis of the relative amount of interacting RC proteins, an amount of membranes corresponding to 80 μg of total membrane protein from NCIB8253 and TB59, containing either plasmid pATP19P or plasmid p6His-C, was solubilized with approximately 50 μL of 50 mM Tris−Cl (pH 8.0) buffer containing 0.5% LDAO, 12.5 mM imidazole, and 1 M NaCl. After centrifugation (2500 RCF, 5 min), the supernatant fluids were bound for 30 min to Ni^{2+}−NTA agarose beads (Qiagen) previously equilibrated with the same buffer as used for solubilization. The beads were washed with three 200 μL portions of the same solution as for solubilization except that the concentration of LDAO was reduced to 0.1%. Bound protein was eluted with three 20 μL portions of 50 mM Tris−Cl (pH 8.0) buffer containing 0.1% LDAO, 250 mM imidazole, and 1 M NaCl. The elutions were pooled and proteins precipitated by diluting 4:1 with ice-cold 100% trichloroacetic acid. Precipitated proteins were washed with acetone, dried, and dissolved in SDS−PAGE sample buffer before analysis in SDS−PAGE and Western blotting.

For large-scale isolation of RCs for absorption spectroscopy and pigment analysis, the isolation was performed as described previously (*29*).

SDS−PAGE and Western Blotting. Isolated membranes with protein amounts stated in the figure captions, as determined by a modified Lowry assay (*30*), were solubilized with sample buffers and run on SDS−PAGE or tricine−SDS−PAGE (*31*). Gels were stained directly with Sypro Ruby protein stain (Invitrogen) and visualized on a Typhoon 9600 scanner (Amersham Biosciences) to reveal protein

bands or electroblotted onto nitrocellulose membranes for probing with antibodies.

Immunodetection of proteins on blots was performed as recommended by the Amersham ECL kit with antibodies raised against purified *Rba. sphaeroides* RC proteins kindly provided by S. Kaplan (University of Texas) and E. Abresch (University of California, San Diego).

Quantification of protein bands detected by antibodies was done by scanning blots on a Versadoc multi-imager station (BioRad), with subsequent pixel analysis of bands using the QuantityOne (BioRad) program to measure the intensity of chemiluminescent light produced.

Absorption Spectroscopy. For investigation of LH and RC complex assembly, purified membranes of *Rba. sphaeroides* grown under low aeration resuspended in 50 mM Tris−Cl (pH 8.0) were analyzed in a Hitachi U-2010 spectrophotometer. Data analysis was done using UV Solutions version 2.1 (Hitachi) and Microsoft Excel. The ratio of LH2 to LH1 was determined by using the peak deconvolution method of Sturgis et al. (*32*), with modification for the *bchD* mutant by substitution of 793, 836, and 859 nm in equations for 800, 850, and 875 nm values, respectively.

The amounts of BChls were determined by absorption spectroscopy of acetone/methanol (7:2) extractions of purified membranes of known protein amount, using $\epsilon = 75$ mM^{-1} cm^{-1} (*33*) at 775 nm (BChl) and estimated $\epsilon = 56.3$ mM^{-1} cm^{-1} at 771 nm (Zn-BChl) (*34*). The presence of quinone in RCs was evaluated using a modification of a previously described method (*35*). Briefly, purified RC samples in 50 mM Tris−Cl (pH 8.0), 0.1% LDAO, and 150 mM imidazole were extracted with methanol/pentane/hexane (3:1:1), and the organic solvent layer was collected, dried under nitrogen, resuspended in ethanol, and analyzed by absorption spectroscopy. The presence of a peak at approximately 275 nm indicated the presence of quinone.

Identification of Zn-BChl. Pigments were extracted from cells with acetone/methanol (7:2), concentrated by vacuum evaporation, and separated by chromatography through a Prodigy ODS-prep column (Phenomenex) attached to a Waters 2695 HPLC instrument fitted with a 200−800 nm photodiode array detector. Pigments were eluted from the column using methanol/water/acetone (16:5:4) for 20 min, followed by acetone/methanol (9:1).

Mass spectrometry of HPLC-purified peak I was performed at the UBC microanalysis and mass spectrometry facility using a biflex IV MALDI-TOF mass spectrometer (Bruker). Briefly, the sample and matrix (*trans*-2-[3-(4-*tert*-butylphenyl)-2-methyl-2-propenylidene]malononitrile (DCTB)) were dissolved in dichloromethane, either with or without acid, mixed in a ratio of 1:1, and 1 μL was applied to the target and dried in air. The sample was run using the reflector mode and pulsed ion extraction.

RESULTS

Amounts of RC and LH Proteins in Membranes from the bchD mutant. We began our study of the magnesium chelatase (*bchD*) mutant by determining the relative amounts of photosystem proteins in the membrane (chromatophore) fraction of cells. Western blotting of RC proteins showed significant amounts of RC H, M, and L in the *bchD* mutant, although at lower levels than in the wild-type strain (Figure 1A). Quantification of the intensity of each band and normalizing *bchD* mutant to wild-type values showed that on average the RC H protein was present at the lowest amount (12% of that of the wild type), RC L was present at 32%, and RC M was present at the highest amount, 46% (Table 1).

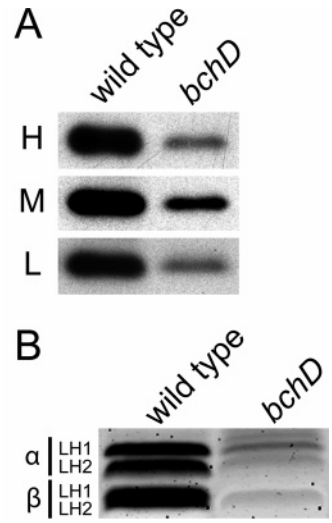

FIGURE 1: Relative amounts of photosystem proteins in wild-type and *bchD* membranes. (A) Western blot of wild-type and *bchD* membranes. Each lane contained 10 μg of membrane proteins. Blots were probed sequentially with anti-RC H/M/L antibodies. (B) Tricine−SDS−PAGE gel of wild-type and *bchD* membranes. Each lane contained 30 μg of membrane proteins.

Table 1: Relative Amounts of Photosystem Proteins in *bchD* Mutant Membranes[a]

protein	amt relative to that of the wild type (%)[b]	protein	amt relative to that of the wild type (%)[c]
RC H	12(5)	LH1/2-α	52(1)
RC M	46(2)	LH1/2-β	14(4)
RC L	32(5)		

[a] Mean of experiments on three independent cultures, with standard deviations in parentheses. [b] Difference between protein band pixel volumes of the wild type and *bchD* mutant in Western blots. [c] Difference between protein band pixel volumes of the wild type and *bchD* mutant from stained tricine−SDS−PAGE gels.

We do not have antibodies to detect LH proteins in Western blots, and so staining of tricine−SDS−PAGE was used to visualize LH1 and LH2 α and β protein bands (Figure 1B). This approach was possible because the LH1 and LH2 α/β proteins are small and well-separated from the rest of the membrane proteins. Quantification of LH band intensities indicated that the aggregate level of LH1 α and LH2 α proteins on average was 52% of that of the wild type, whereas the β proteins were present at 14% of that of the wild type (Table 1).

RC Proteins Form a Complex in the bchD Mutant. The possibility that RC proteins interact to form a complex in the *bchD* mutant was evaluated using a six-histidine (6His) tag pull-down approach. A plasmid expressing the *puhA* (RC H) gene modified by addition of a C-terminal 6His tag was introduced into *bchD* and wild-type strains. Membrane proteins were solubilized with LDAO detergent, bound to Ni^{2+}−NTA beads, and eluted with imidazole (see the Materials and Methods). Western blot analysis of the elutions

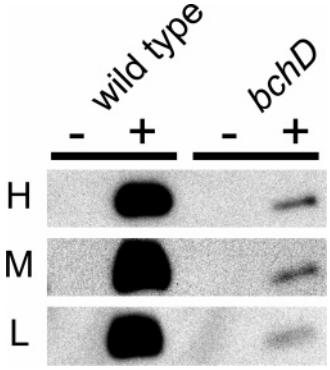

FIGURE 2: Relative amounts of interacting RC proteins in wild-type and *bchD* membranes. Western blot of 6His-tagged RC H pull-down elutions from wild-type and *bchD* solubilized membranes from cells containing either empty vector pATP19P (−) or p6His-C with RC H (*puhA*) gene encoding six C-terminal histidines (+). Equal amounts of membrane proteins from each strain (80 μg) were solubilized and mixed with Ni^{2+}−NTA beads.

Table 2: Relative Amounts of RC Proteins Pulled Down by 6His-Tagged RC H[a]

protein	amt relative to that of the wild type (%)
RC H	7(3)
RC M	12(6)
RC L	16(3)

[a] Difference between protein band pixel volumes of wild-type and *bchD* mutant elutions in Western blots. Mean of experiments on three independent cultures, with standard deviations in parentheses.

showed that all three RC proteins coeluted from the Ni^{2+}−NTA beads incubated with solubilized membrane proteins from either *bchD* or wild-type cells expressing the 6His-tagged RC H, whereas none of the RC proteins were seen in the elutions of material from cells lacking the 6His-tagged RC H protein (Figure 2). No dissociation of RC complexes in wild-type or *bchD* samples was seen during the pull-down procedure. This coelution of all three RC proteins indicates that the RC M and L proteins bind to RC H in *bchD* mutant cell membranes and therefore form a complex.

RC protein band intensities were quantified, and the data in Table 2 show that the average amounts of RC H, M, and L that copurified from the *bchD* mutant were 7−16% of the wild-type values. The amounts of RC M and L relative to RC H were significantly lower in the pull-downs than in membranes of cells (compare Tables 1 and 2), because only RC M and L proteins that bind to the introduced 6His-tagged RC H protein are bound to the Ni^{2+}−NTA beads. Therefore, the amount of RC M and L seen in Figure 2 should be approximately equal to the amount of RC H in the mutant. These data indicate that the majority of RC H in the mutant is bound in RC complexes whereas RC M and RC L are present in excess.

LH and RC Complexes in the bchD Mutant Contain a BChl-like Pigment. To determine whether pigments were assembling with LH proteins in *bchD* mutant membranes, absorption spectra of chromatophores from cells grown to the stationary phase under low aeration were measured. In the wild-type strain, characteristic absorption peaks in the 450−500 nm region indicate the presence of carotenoids and peaks in the 800−875 nm region indicate the presence of

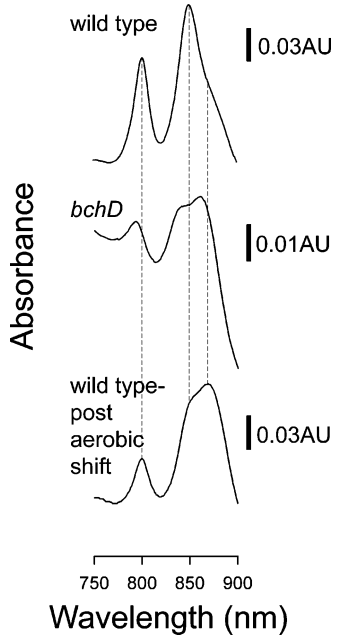

FIGURE 3: Comparison of LH complex absorption between wild type and *bchD* mutant membranes. Absorption spectra of chromatophores from wild-type (top) and *bchD* (middle) cells grown to the stationary phase under low aeration and wild-type cells 8 h after transition from photosystem-repressing (high aeration) to photosystem-inducing (low aeration) conditions (bottom). Vertical dotted lines denote positions of wild-type peak maxima. Spectra were normalized to absorbance at 650 nm.

BChl bound to LH complexes. Surprisingly, in addition to the presence of carotenoid peaks (data not shown), the absorption spectrum of the *bchD* mutant revealed peaks at 793, 836, and 859 nm, which are blue-shifted 7−16 nm compared to the corresponding wild-type LH2 peaks at 800 and 850 nm and the LH1 peak at 875 nm (Figure 3, top two traces). These data indicate that LH1 and LH2 complexes assemble in the *bchD* mutant, but bind a pigment that differs from the BChl found in complexes from identically grown wild-type cells. Interestingly, when grown under low aeration conditions, the LH2:LH1 peak ratio (0.50) of the putative *bchD* mutant complexes differs from the ratio (1.48) in identically grown wild-type cells and is instead closer to the ratio (0.41) in wild-type cells at an early stage (8 h) after shifting from high aeration (photosystem-repressing) to low aeration (photosystem-inducing) growth conditions (Figure 3, bottom trace).

Following up on the discovery that LH complexes in the *bchD* mutant appear to bind a BChl-like pigment, a similar spectral analysis was performed on the RC. Because RC absorption peaks are hidden by the LH peaks in chromatophores, we purified RC complexes from wild-type and *bchD* cells. The absorption spectra of RC complexes purified from the wild type and *bchD* mutant were similar, with both preparations yielding distinct peaks in the 700−900 nm region and overlapping peaks in the 450−500 nm region (Figure 4A). However, there were three major differences between these RCs: (1) the BChl special pair peak, at 865 nm in the wild-type strain, was blue-shifted to 855 nm in the *bchD* mutant; (2) the accessory BChl peak, at 803 nm in the wild type, was shifted to 795 nm in the *bchD* mutant; (3) the *bchD* mutant spectrum lacked a peak at 760 nm corresponding to BPhe absorption in the wild-type RC (*36*).

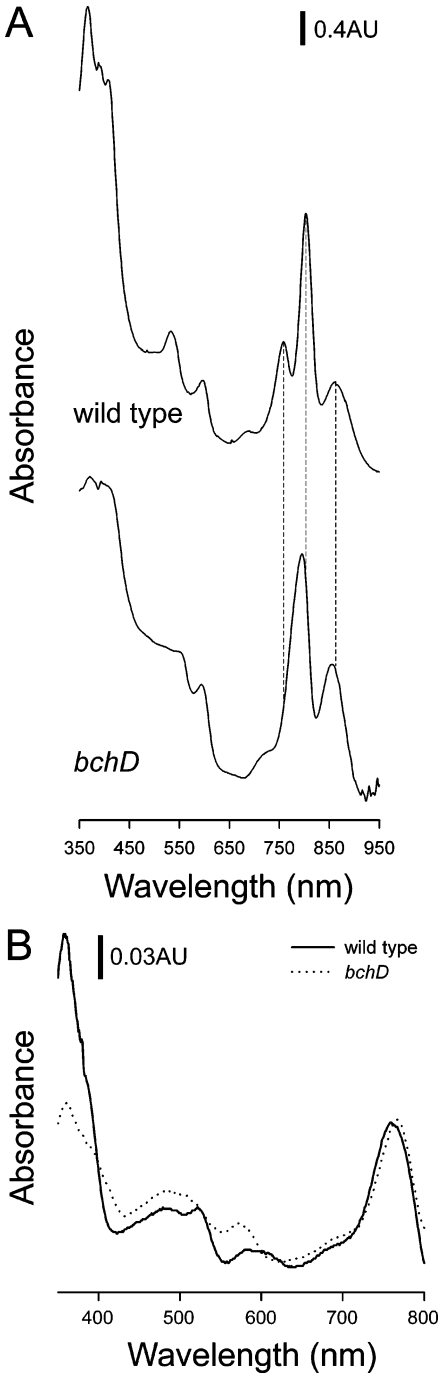

FIGURE 4: Comparison of RC composition between the wild type and *bchD* mutant. (A) Absorption spectra of purified RC complexes isolated using His-tagged RC H. Vertical dotted lines denote positions of wild-type peak maxima. (B) Absorption spectra of acetone/methanol extraction of RCs.

To better understand the nature of the pigments bound to the RC from the *bchD* mutant, the purified RC was extracted with acetone/methanol (7:2). The absorption spectrum of pigments extracted from the *bchD* RC showed a major far-red peak at 766 nm, whereas pigments extracted from the wild-type RC absorbed maximally in the far-red region at 759 nm (Figure 4B). The wild-type peak results from the combined absorption of a 2:1 ratio of BChl (771 nm) to BPhe (750 nm) (*33*). However, the absorption spectrum of the *bchD* RC (see above) indicates that it lacks BPhe, and this finding is supported by the lack of the BPhe Q_x band in the extract spectrum at approximately 525 nm (*34*). Therefore, the extracted BChl-like pigment appears to have an absorption peak at 766 nm, blue-shifted by 5 nm relative to that of BChl.

The absorption peaks in the 450−500 nm region show the presence of carotenoid in the *bchD* RC. Additional extractions of purified RCs with other solvents (see the Materials and Methods) indicated the presence of quinone in the *bchD* RC (data not shown). Thus, the *bchD* mutant assembles an RC that contains a BChl-like pigment, carotenoid, and quinone, but lacks BPhe.

Isolation of the BChl-like Pigment from bchD Cells and Identification as Zn-BChl. Because of the small quantity of pigment available for extraction from purified RCs, larger scale extractions from cells of wild-type and *bchD* mutant strains were separated by HPLC to investigate the differences in pigment composition (Figure 5A). As expected, BChl was the major component in the wild-type elution profile (retention time of 19.2 min), with a lesser amount of BPhe (retention time of 21.1 min). The peak at 20.4 min is attributed to carotenoid, on the basis of the absorption spectrum. The absorption spectrum of BChl yielded major peaks at 364, 600, and 770 nm (Figure 5B).

The *bchD* mutant elution profile lacked BChl and BPhe peaks, although the carotenoid peak at 20.4 min was present. The major pigment eluted at 19.7 min and is labeled as peak I in Figure 5A. Peak I had an absorption spectrum similar to that of BChl, but with blue-shifted peaks at 357, 569, and 766 nm (Figure 5B), which match those of the BChl-like pigment extracted from the *bchD* RC (Figure 4B).

The material in peak I was subjected to MALDI-TOF mass spectrometry analysis to evaluate the identity of the pigment (Figure 5C). The mass to charge ratio (*m*/*z*) of the predominant peak was 950.6, which differs from the predicted BChl *m*/*z* of 911.5. However, the *m*/*z* of peak I (950.6) agrees well with the predicted *m*/*z* (950.5) of BChl that contains zinc instead of magnesium (called Zn-BChl on the basis of the proposed nomenclature (*37*); see Figure 5D). When peak I material was analyzed in mass spectrometry using an acidic matrix to remove chelated metal, the 950.6 *m*/*z* peak amplitude decreased and a new peak appeared at *m*/*z* 886.5 (data not shown), which corresponds to the mass of BChl lacking a metal (i.e., BPhe). Further evidence for the identification of peak I as Zn-BChl comes from the ratio between the 950.6 peak and the seven adjacent peaks with larger *m*/*z* numbers (seen in the inset of Figure 5C), which correspond to those predicted for naturally occurring isotopes of zinc.

We suggest that the *bchD* mutant assembles a novel RC that contains Zn-BChl in place of the special pair and accessory BChls, but lacks BPhe in the $H_{A,B}$ sites. Furthermore, on the basis of the relative RC peak amplitudes in the absorption spectrum, we suggest that the $H_{A,B}$ sites lack a chlorin of any kind.

The bchD Mutant Assembles Lower Amounts of LH and RC Complexes Than the Wild-Type Strain Because of Low Levels of Zn-BChl. The experiments described above indicate low levels of LH and RC proteins and complexes in the *bchD* mutant and that the blue shifts of the absorption peaks relative to those of the wild-type strain are due to the substitution of Zn-BChl for BChl in the LH and RC complexes (Figures 3−5).

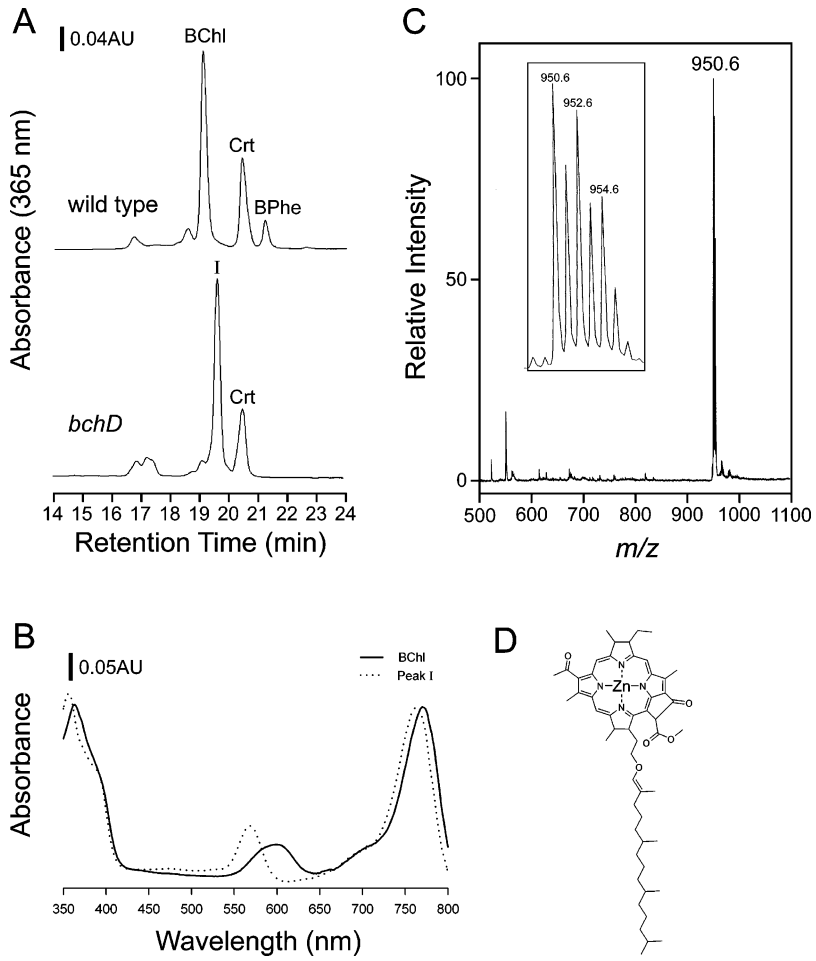

FIGURE 5: Isolation and identification of BChl-like pigment from the *bchD* mutant. (A) HPLC trace of wild-type (top) and *bchD* (bottom) whole cell acetone/methanol extractions. Crt, carotenoid; BChl, bacteriochlorophyll; BPhe, bacteriopheophytin. (B) Absorption spectra of the BChl peak from the wild type and peak I from the *bchD* mutant in acetone/methanol solvent. (C) Mass spectrometry analysis of peak I. Inset: magnified view of the 950.6 *m*/*z* region. (D) Proposed structure of peak I.

To investigate the limiting factor for photosystem assembly in the *bchD* mutant, we compared absorption peak amplitudes of chromatophores from mutant and wild-type cells grown under identical, low aeration conditions. Although the extinction coefficient of Zn-BChl in acetone/methanol or in vivo has not been determined, we assume that it is approximately 25% lower than that of BChl, on the basis of values previously determined in pyridine and diethyl ether (*34*). The data indicate that *bchD* cells develop 4−6% of the LH2 and 7% of the LH1 complexes relative to those of the wild-type strain (Figure 6A). These values are similar to the relative amounts of BChls, about 5% Zn-BChl in the *bchD* mutant compared to the amount of BChl in the wild-type strain (Figure 6B), but significantly less than the individual amounts of RC proteins (12−46% of the wild-type levels) and LH proteins (14−52% of the wild-type levels) would potentially allow (Table 1).

Attempts to boost expression of the Zn-BChl-containing RC were undertaken by increasing the Zn^{2+} concentration of the growth medium. Initial experiments showed no increase in Zn-BChl or RC complex assembly with increased Zn^{2+} concentration. Further experiments manipulating the pH and Fe^{2+} or Zn^{2+} concentration of the growth medium are currently under way.

Thus, it appears that the production of Zn-BChl is the limiting factor in the assembly of LH and RC complexes in *bchD* mutant cells. The small amount of Zn-BChl produced in the cell combined with the *bchD* mutant's photosynthetic-negative phenotype are likely reasons why the novel photosystem described in this paper was overlooked in the initial characterization of this mutant (*23*).

DISCUSSION

As far as we know, this is the first report of Zn-BChl produced in a purple photosynthetic bacterium that normally assembles LH and RC complexes containing BChl. It may appear surprising that this was discovered in a mutant lacking the enzyme of the first step in the BChl biosynthetic pathway, but we suggest below that the absence of a functional magnesium chelatase is a major factor in both the synthesis and detection of Zn-BChl.

There are two other cases where Zn^{2+} is substituted for Mg^{2+} in chlorins in vivo. One is the unicellular alga *Chlorella kessleri*, which produces zinc chlorophyll only when grown heterotrophically to the late stationary phase in acidic media containing more than 2000 times the usual concentration of Zn^{2+} (>16.8 mM) (*38*). The second case is the purple phototrophic acidophile *Acidiphilium rubrum* (*39*), which assembles RC and LH1 complexes exclusively with Zn-BChl. In both cases, the organisms grow under acidic conditions, possess functional magnesium chelatases, and are believed to produce Zn-(B)Chl after normal (B)Chl biosyn-

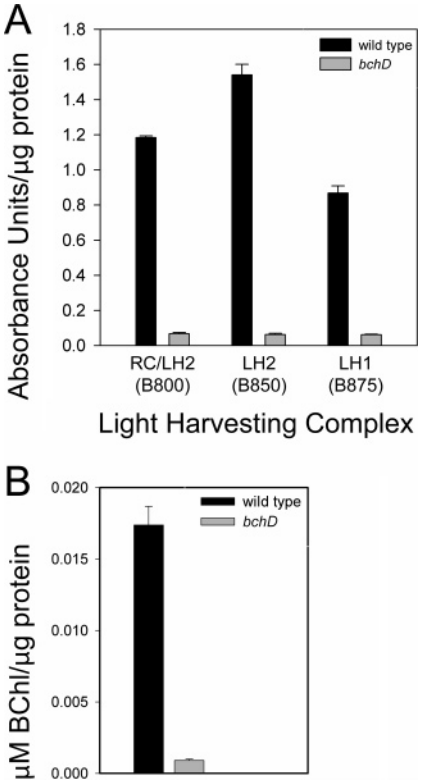

FIGURE 6: Comparison of photosystem assembly and (Zn-)BChl content of wild-type and *bchD* membranes. (A) Comparison of LH1 and LH2 assembly. Amounts of LH complexes determined by absorption spectra of membranes using LH2 and LH1 peaks measured at 800, 850, and 875 nm for the wild type and 793, 836, and 859 nm for the *bchD*, mutant respectively. (B) Comparison of total (Zn-)BChl amounts. BChls quantified using absorption at 775 nm for BChl and 771 nm for Zn-BChl, assuming $\epsilon = 75$ mM^{-1} cm^{-1} for BChl and $\epsilon = 56.3$ mM^{-1} cm^{-1} for Zn-BChl.

thesis (*38*, *40*). These cases are in contrast to the *bchD* mutant, which grows at neutral pH where Zn^{2+} is less soluble and synthesizes Zn-BChl without first producing BChl.

Possible Zn-BChl Biosynthetic Pathways. Although the possibility that the *bchD* mutant's magnesium chelatase could somehow chelate Zn^{2+} into PPIX cannot be dismissed, we propose instead that Zn-BChl is created in these cells from zinc protoporphyrin IX (Zn-PPIX) as a byproduct of the ferrochelatase-catalyzed insertion of Fe^{2+} into PPIX to create heme. It has been known for some time that ferrochelatase, given favorable conditions in vitro, inserts Zn^{2+} into PPIX at approximately 75% the rate of Fe^{2+} insertion (*41*). Evidence for the in vivo presence of this byproduct comes from reports of small quantities of Zn-PPIX in *Cyanidium caldarium* (*42*) and in yeast, with the amount of Zn-PPIX found increasing in strains with disruptions of their normal porphyrin metabolism (*43*).

Because the *bchD* mutant lacks a functional magnesium chelatase, the cellular amounts of PPIX are expected to increase significantly, as observed in a *Rba. capsulatus bchD* mutant (*44*). We speculate that the amount of iron in the *bchD* mutant is the same as in the wild-type strain, but the amount of PPIX substrate for ferrochelatase is elevated, thereby increasing the chance of Zn^{2+} rather than Fe^{2+} addition to PPIX. The Zn-PPIX that is produced as a byproduct of heme synthesis in the *bchD* mutant is acted on by the second enzyme of the BChl biosynthetic pathway, BchM, which normally catalyzes the methylation of the 13-propionate side chain of magnesium protoporphyrin IX (*45*). After methylation of Zn-PPIX by BchM, Zn-containing intermediates proceed through the normal BChl biosynthetic pathway, yielding Zn-BChl. This scheme is plausible because it was reported that enzymes in the later stages of chlorophyll biosynthesis tolerate changes in the centrally chelated metal as long as it is pentacoordinated square-pyramidal, as are Zn^{2+} and Mg^{2+} (*46*).

Levels and Assembly of LH and RC Complexes in the bchD Mutant. The reduced pool of RC and LH proteins in the *bchD* mutant may result from a combination of a shortage of Zn-BChl, reducing the amount of complexes assembled, as well as the degradation of noncomplexed proteins. Previous work showed that the absence of BChl decreases the steady-state levels of LH and RC proteins in the ICM, presumably because of degradation of noncomplexed proteins (*17*, *18*). Furthermore, pulse-chase experiments on a *Rba. capsulatus bchH* mutant showed loss of LH proteins from the ICM fraction, with the LH1/2 β proteins lost at a faster rate than the LH1/2 α proteins (*18*). This differential stability is consistent with the LH protein levels seen in the *bchD* mutant (Table 1), where the relative amounts of α proteins were greater than those of the β proteins. Another interesting finding is that the RC protein amounts (M > L > H) in the *bchD* mutant follow the same pattern as the proposed stabilities determined from RC single-gene knockouts (*47*), which may be due to the inherent stabilities of the noncomplexed proteins.

Although Zn-BChl incorporation into an LH1-type complex was reported for *A. rubrum* (*39*), the presence of Zn-BChl in the *Rba. sphaeroides* LH2-type complex described in this paper is new. In the *bchD* mutant the LH2 complex accumulates to a lesser extent than LH1 due to preferential targeting of limited amounts of Zn-BChl to the LH1 complex, inefficient assembly of the LH2 complex with Zn-BChl, or decreased stability of the LH2 complex. The low ratio of LH2 to LH1 in the *bchD* mutant resembles the ratio in wild-type cells when low amounts of BChl limit photosystem development. In wild-type cultures undergoing a shift from high to low aeration, when BChl production first begins, the core RC−LH1 complex is assembled first, followed by the LH2 complex later in the maturation process (*48*). More relevant to the *bchD* mutant steady-state situation are the results obtained with *Rba. sphaeroides* ALA synthase mutants (*49*). For ALA synthase mutants to produce BChl, they must be fed exogenous ALA, allowing the modulation of the amount of BChl produced. When only small amounts of ALA were given to the cells, limiting BChl production, the LH2:LH1 ratios were similar to what was seen for the *bchD* mutant (*49*). Our work is consistent with a model of photosystem assembly proposed in previous studies of cells under BChl-limiting conditions because the *bchD* mutant, with Zn-BChl at 5% of the wild-type BChl level (Figure 6B), contains a greater ratio of RC−LH1 core complex to LH2 complex than the wild-type strain (Figures 3 and 6A).

Effects of Zn-BChl on the Assembly and Properties of the RC. The copurification of RC proteins using a 6His tag on the RC H protein shows that the H, M, and L proteins form a complex in the *bchD* mutant (Figure 2), and therefore, Zn-BChl functions in place of BChl for in vivo assembly of the *Rba. sphaeroides* RC. Furthermore, the absence of BPhe in the *bchD* mutant shows that BPhe is not needed for the in

vivo assembly of an RC that contains the other cofactors. However, the *bchD* RC is incapable of supporting photosynthetic growth (*23*) (data not shown), probably because electron transfer from the special pair to Q_A cannot take place in the complete absence of BPhe.

Past work on *Rba. sphaeroides* RCs reconstituted in vitro with Zn-BChl derivatives bound to the $B_{A,B}$ sites indicated no significant changes in the binding, relative to that of BChl (*50*). In another study Zn-BChl was reconstituted into the *Rba. sphaeroides* RC $P_{A,B}$ (special pair) and $B_{A,B}$ (accessory BChl) sites, although only 30% occupancy was achieved. The absorption spectra of these partially reconstituted RCs yielded peaks at 864 nm for the special pair and 800 nm for the accessory BChls (*51*). These values differ from those of the peaks attributed to the special pair (855 nm) and the accessory BChls (795 nm) in the RC purified from the *bchD* mutant and in fact more closely resemble those of the wild-type RC peaks. The discrepancy may be due to the low occupancy of Zn-BChl and incomplete removal of BChl in the reconstituted RCs in the other work (*51*).

In contrast, the RC isolated from *A. rubrum*, which has RC proteins homologous to those of *Rba. sphaeroides* but assembles normally with four Zn-BChls in vivo (*52*), has an absorption spectrum more similar to that of the *bchD* RC: the *A. rubrum* special pair peak is at 859 nm (vs 855 nm for the *bchD* RC), and the accessory BChl's peak is at 792 nm (vs 795 nm). Evidently these absorption peak differences reflect amino acid sequence differences in the RC proteins. It was suggested that the difference in the amino acid at position L168 between *Rba. sphaeroides* (His) and *A. rubrum* (Glu) changes the electronic character of the special pair, allowing the *A. rubrum* RC with Zn-BChl to function similarly to the *Rba. sphaeroides* native RC (*52*). Experiments on an L168 His → Glu *Rba. sphaeroides* mutant RC showed a weakening or flattening of the special pair absorption peak compared to that of the native RC, similar to that seen in *A. rubrum* (*52*, *53*). Our results support the idea that residue L168 affects the electronic coupling of the special pair, because the special pair to accessory BChl peak ratio in the *bchD* RC is more similar to that in the *Rba. sphaeroides* native RC than the *A. rubrum* RC.

Absence of BPhe from bchD Cells. The reason for the absence of BPhe from *bchD* mutant RCs is unknown, although it must be linked to the substitution of Zn for Mg in the macrocycle. Because Zn-BChl is much more resistant to pheophytinization (dechelation) than is BChl (*54*), this property is likely responsible for the absence of BPhe. Several possible dechelating activities in the cell that could be affected by the increased strength of Zn^{2+} vs Mg^{2+} binding to the chlorin macrocycle include the RC itself, a dedicated dechelatase enzyme, or a spontaneous process.

We note that the only cellular location for BPhe is the RC complex and that previous work on the RC suggests that it may function as a BChl dechelatase. Site-directed mutation of RC His residues (which bind to the Mg^{2+} of BChl) to Leu resulted in the substitution of BPhe in place of special pair BChls (*55*). Converse changes to other RC residues resulted in the substitution of BChl in place of BPhe in the $H_{A,B}$ sites or the absence of a chlorin at the H_B site (*21*, *22*). When key amino acid (RC L173,185; RC M202,214) side chains on the RC M and L proteins are large nonpolar moieties, such as Leu, a BPhe is bound. Alternatively, when the same residue has instead a polar side chain, typically His, a BChl is bound (*21*, *22*, *55*). A unifying explanation derived from these previous results is that key amino acid side chains that project toward the center of the chlorin macrocycle either bind (His residue) or dechelate (Leu residue) the Mg from BChl. We speculate that the reason why there is no BPhe found in the *bchD* mutant RC is because the binding strength of Zn^{2+} in the BChl macrocycle is greater than the affinity of the macrocycle for the RC H_A and H_B pockets. The *bchD* RC provides a tool to test the proposed dechelatase activity of the RC because of the complete absence of bound BPhe. In vitro reconstitution experiments (*56*) with BChl and Zn-BChl could determine whether the *bchD* RC alone is sufficient to generate and bind BPhe using BChl as the substrate.

An alternative explanation for the lack of BPhe is the possibility of a dedicated dechelatase enzyme in *Rba. sphaeroides* that is unable to remove the strongly bound Zn^{2+} from Zn-BChl. Another possibility is that the disrupted magnesium chelatase enzyme itself has a role in the dechelation reaction, although this seems less likely because of the differing structures of PPIX and BChl. Finally, a nonenzymatic route to generating BPhe is possible which would be hampered by the increased binding strength of Zn^{2+} to the chlorin and neutral pH of the growth conditions used in our work.

We note that both organisms previously found to make Zn-(B)Chl also make Mg-(B)Chl and (B)Phe, which is distinct from the situation found in the *bchD* strain. Because *A. rubrum* and *C. kessleri* can presumably make (B)Phe from Mg-(B)Chl, they do not have to dechelate the Zn-(B)Chl derivative. In fact, this (B)Phe molecule has been suggested by both groups as a possible intermediate in the synthesis of Zn-(B)Chl (*38*, *40*).

SUMMARY

This paper reports several new characteristics of a magnesium chelatase subunit D (*bchD*) mutant strain of *Rba. sphaeroides* that we found creates Zn-BChl, and assembles it into RC and LH complexes. How this pigment is synthesized by the cell is currently unknown, but it may be an unusual example of a side reaction catalyzed by an enzyme (ferrochelatase) producing a substrate (Zn-PPIX) that is able to feed into an otherwise normal biosynthetic pathway.

The reason why the *bchD* mutant is unable to make BPhe from Zn-BChl is unclear, but we suggest that the greater stability of Zn-BChl relative to BChl is a barrier to removal of Zn^{2+} from the macrocycle by the RC or other dechelatase activity in the cell. Perhaps this work will spur new investigations into the origin of the BPhe molecule. The RC assembles in *bchD* mutant cells without both of the BPhes, so BPhe is not needed for RC assembly. The *bchD* mutant has potential in the study of LH and RC complex assembly, structure, and function with BChls containing a variety of metals, if this mutant can be coaxed to take up and process exogenously supplied metalloprotoporphyrins IX through the BChl biosynthetic pathway.

ACKNOWLEDGMENT

We thank C. N. Hunter for providing the TB59 (*bchD*) strain, S. Kaplan and E. Abresch for providing antisera, M.

Paddock for purified *Rba. sphaeroides* RC, L. Eltis for use of the Typhoon and HPLC instruments, and the UBC microanalysis facility for mass spectrometry.

REFERENCES

1. Zeilstra-Ryalls, J., Gomelsky, M., Eraso, J. M., Yeliseev, A., O'Gara, J., and Kaplan, S. (1998) Control of photosystem formation in *Rhodobacter sphaeroides*, *J. Bacteriol. 180*, 2801−2809.
2. Chory, J., Donohue, T. J., Varga, A. R., Staehelin, L. A., and Kaplan, S. (1984) Induction of the photosynthetic membranes of *Rhodopseudomonas sphaeroides*-biochemical and morphological studies, *J. Bacteriol. 159*, 540−554.
3. Okamura, M. Y., Paddock, M. L., Graige, M. S., and Feher, G. (2000) Proton and electron transfer in bacterial reaction centers, *Biochim. Biophys. Acta 1458*, 148−163.
4. Qian, P., Hunter, C. N., and Bullough, P. A. (2005) The 8.5 angstrom projection structure of the core RC-LH1-PufX dimer of *Rhodobacter sphaeroides*, *J. Mol. Biol. 349*, 948−960.
5. Scheuring, S., Busselez, J., and Levy, D. (2005) Structure of the dimeric PufX-containing core complex of *Rhodobacter blasticus* by *in situ* atomic force microscopy, *J. Biol. Chem. 280*, 1426−1431.
6. Scheuring, S., Francia, F., Busselez, J., Melandri, B. A., Rigaud, J. L., and Levy, D. (2004) Structural role of PufX in the dimerization of the photosynthetic core complex of *Rhodobacter sphaeroides*, *J. Biol. Chem. 279*, 3620−3626.
7. Bahatyrova, S., Frese, R. N., Siebert, C. A., Olsen, J. D., van der Werf, K. O., van Grondelle, R., Niederman, R. A., Bullough, P. A., Otto, C., and Hunter, C. N. (2004) The native architecture of a photosynthetic membrane, *Nature 430*, 1058−1062.
8. Cogdell, R. J., Isaacs, N. W., Freer, A. A., Howard, T. D., Gardiner, A. T., Prince, S. M., and Papiz, M. Z. (2003) The structural basis of light-harvesting in purple bacteria, *FEBS Lett. 555*, 35−39.
9. Lancaster, C. R. D., Ermler, U., and Michel, H. (1995) The Structures of Photosynthetic Reaction Centers from Purple Bacteria as Revealed by X-Ray Crystallography, in *Advances in Photosynthesis: Anoxygenic Photosynthetic Bacteria* (Blankenship, R. E., Madigan, M. T., and Bauer, C. E., Eds.) pp 503−526, Kluwer Academic Publishers, Dordrecht, The Netherlands.
10. Beale, S. I. (1995) Biosynthesis and Structures of Porphyrins and Hemes, in *Advances in Photosynthesis: Anoxygenic Photosynthetic Bacteria* (Blankenship, R. E., Madigan, M. T., and Bauer, C. E., Eds.) pp 153−159, 162−169, Kluwer Academic Publishers, Dordrecht, The Netherlands.
11. Gibson, L. C. D., Willows, R. D., Kannangara, C. G., von Wettstein, D., and Hunter, C. N. (1995) Magnesium-protoporphyrin chelatase of *Rhodobacter sphaeroides*: reconstitution of activity by combining the products of the *bchH*, *-I*, and *-D* genes expressed in *Escherichia coli*, *Proc. Natl. Acad. Sci. U.S.A. 92*, 1941−1944.
12. Suzuki, J. Y., Bollivar, D. W., and Bauer, C. E. (1997) Genetic analysis of chlorophyll biosynthesis, *Annu. Rev. Genet. 31*, 61−89.
13. Brown, A. E., Eiserlin, F. A., and Lascelles, J. (1972) Bacteriochlorophyll synthesis and ultrastructure of wild-type and mutant strains of *Rhodopseudomonas spheroides*, *Plant Physiol. 50*, 743−746.
14. Zhang, H. T., Li, J. J., Yoo, J. H., Yoo, S. C., Cho, S. H., Koh, H. J., Seo, H. S., and Paek, N. C. (2006) Rice chlorina-1 and chlorina-9 encode ChlD and ChlI subunits of Mg-chelatase, a key enzyme for chlorophyll synthesis and chloroplast development, *Plant Mol. Biol. 62*, 325−337.
15. Eichacker, L. A., Soll, J., Lauterbach, P., Rüdiger, W., Klein, R. R., and Mullet, J. E. (1990) *In vitro* synthesis of chlorophyll *a* in the dark triggers accumulation of chlorophyll *a* apoproteins in barley etioplasts, *J. Biol. Chem. 265*, 13566−13571.
16. Mullet, J. E., Klein, P. G., and Klein, R. R. (1990) Chlorophyll regulates accumulation of the plastid-encoded chlorophyll apoprotein-Cp43 and apoprotein-D1 by increasing apoprotein stability, *Proc. Natl. Acad. Sci. U.S.A. 87*, 4038−4042.
17. Varga, A. R., and Kaplan, S. (1993) Synthesis and stability of reaction center polypeptides and implications for reaction center assembly in *Rhodobacter sphaeroides*, *J. Biol. Chem. 268*, 19842−19850.
18. Brand, M., and Drews, G. (1997) The role of pigments in the assembly of photosynthetic complexes in *Rhodobacter capsulatus*, *J. Basic Microbiol. 37*, 235−244.
19. Papenbrock, J., Pfundel, E., Mock, H. P., and Grimm, B. (2000) Decreased and increased expression of the subunit CHL I diminishes Mg chelatase activity and reduces chlorophyll synthesis in transgenic tobacco plants, *Plant J. 22*, 155−164.
20. Takemoto, J., and Lascelles, J. (1973) Coupling between bacteriochlorophyll and membrane protein synthesis in *Rhodopseudomonas spheroides*, *Proc. Natl. Acad. Sci. U.S.A. 70*, 799−803.
21. Watson, A. J., Fyfe, P. K., Frolov, D., Wakeham, M. C., Nabedryk, E., van Grondelle, R., Breton, J., and Jones, M. R. (2005) Replacement or exclusion of the B-branch bacteriopheophytin in the purple bacterial reaction centre: the H_B cofactor is not required for assembly or core function of the *Rhodobacter sphaeroides* complex, *Biochim. Biophys. Acta 1710*, 34−46.
22. Kirmaier, C., Gaul, D., Debey, R., Holten, D., and Schenck, C. C. (1991) Charge separation in a reaction center incorporating bacteriochlorophyll for photoactive bacteriopheophytin, *Science 251*, 922−927.
23. Coomber, S. A., Chaudhri, M., Connor, A., Britton, G., and Hunter, C. N. (1990) Localized transposon Tn5 mutagenesis of the photosynthetic gene cluster of *Rhodobacter sphaeroides*, *Mol. Microbiol. 4*, 977−989.
24. Tehrani, A., Prince, R. C., and Beatty, J. T. (2003) Effects of photosynthetic reaction center H protein domain mutations on photosynthetic properties and reaction center assembly in *Rhodobacter sphaeroides*, *Biochemistry 42*, 8919−8928.
25. Bovallius, Å., and Zacharias, B. (1971) Variations in the metal content of some commercial media and their effect on microbial growth, *Appl. Microbiol. 22*, 260−262.
26. Abresch, E. C., Axelrod, H. L. A., Beatty, J. T., Johnson, J. A., Nechushtai, R., and Paddock, M. L. (2005) Characterization of a highly purified, fully active, crystallizable RC-LH1-PufX core complex from *Rhodobacter sphaeroides*, *Photosynth. Res. 86*, 61−70.
27. Keller, S., Beatty, J. T., Paddock, M., Breton, J., and Leibl, W. (2001) Effect of metal binding on electrogenic proton transfer associated with reduction of the secondary electron acceptor (Q_B) in *Rhodobacter sphaeroides* chromatophores, *Biochemistry 40*, 429−439.
28. Simon, R., Priefer, U., and Puhler, A. (1983) A broad host range mobilization system for *in vivo* genetic engineering transposon mutagenesis in gram-negative bacteria, *Bio/Technology 1*, 784−791.
29. Goldsmith, J. O., and Boxer, S. G. (1996) Rapid isolation of bacterial photosynthetic reaction centers with an engineered polyhistidine tag, *Biochim. Biophys. Acta 1276*, 171−175.
30. Peterson, G. L. (1983) Determination of total protein, *Methods Enzymol. 91*, 95−119.
31. Schagger, H., and von Jagow, G. (1987) Tricine sodium dodecyl sulfate-polyacrylamide gel electrophoresis for the separation of proteins in the range from 1 to 100 kDa, *Anal. Biochem. 166*, 368−379.
32. Sturgis, J. N., Hunter, C. N., and Niederman, R. A. (1988) Spectra and extinction coefficients of near-infrared absorption bands in membranes of *Rhodobacter sphaeroides* mutants lacking light-harvesting and reaction center complexes, *Photochem. Photobiol. 48*, 243−247.
33. Clayton, R. K. (1966) Spectroscopic analysis of bacteriochlorophyll *in vitro* and *in vivo*, *Photochem. Photobiol. 5*, 669−677.
34. Hartwich, G., Fiedor, L., Simonin, I., Cmiel, E., Schafer, W., Noy, D., Scherz, A., and Scheer, H. (1998) Metal-substituted bacteriochlorophylls. 1. Preparation and influence of metal and coordination on spectra, *J. Am. Chem. Soc. 120*, 3675−3683.
35. Kroger, A. (1978) Determination of contents and redox states of ubiquinone and menaquinone, *Methods Enzymol. 53*, 579−591.
36. Woodbury, N. W., and Allen, J. P. (1995) Electron Transfer in Purple Nonsulfur Bacteria, in *Advances in Photosynthesis: Anoxygenic Photosynthetic Bacteria* (Blankenship, R. E., Madigan, M. T., and Bauer, C. E., Eds.) pp 527−557, Kluwer Academic Publishers, Dordrecht, The Netherlands.
37. Takaichi, S., Wakao, N., Hiraishi, A., Itoh, S., and Shimada, K. (1999) Nomenclature of metal-substituted (bacterio)chlorophylls in natural photosynthesis: Metal-(bacterio)chlorophyll and M-(B)-Chl, *Photosynth. Res. 59*, 255−256.
38. Ikegami, I., Nemoto, A., and Sakashita, K. (2005) The formation of Zn-Chl *a* in *Chlorella* heterotrophically grown in the dark with an excessive amount of Zn^{2+}, *Plant Cell Physiol. 46*, 729−735.

39. Wakao, N., Yokoi, N., Isoyama, N., Hiraishi, A., Shimada, K., Kobayashi, M., Kise, H., Iwaki, M., Itoh, S., Takaichi, S., and Sakurai, Y. (1996) Discovery of natural photosynthesis using Zn-containing bacteriochlorophyll in an aerobic bacterium *Acidiphilium rubrum*, *Plant Cell Physiol. 37*, 889−893.
40. Masuda, T., Inoue, K., Masuda, M., Nagayama, M., Tamaki, A., Ohta, H., Shimada, H., and Takamiya, K.-i. (1999) Magnesium insertion by magnesium chelatase in the biosynthesis of zinc bacteriochlorophyll *a* in an aerobic acidophilic bacterium *Acidiphilium rubrum*, *J. Biol. Chem. 274*, 33594−33600.
41. Neuberger, A., and Tait, G. H. (1964) Studies on the biosynthesis of porphyrin and bacteriochlorophyll by *Rhodopseudomonas spheroides*, *Biochem. J. 90*, 607−616.
42. Csatorday, K., Maccoll, R., and Berns, D. S. (1981) Accumulation of protoporphyrin IX and Zn protoporphyrin IX in *Cyanidium caldarium*, *Proc. Natl. Acad. Sci. U.S.A. 78*, 1700−1702.
43. Pretlow, T. P., and Sherman, F. (1967) Porphyrins and zinc porphyrins in normal and mutant strains of yeast, *Biochim. Biophys. Acta 148*, 629−644.
44. Bollivar, D. W., Suzuki, J. Y., Beatty, J. T., Dobrowolski, J. M., and Bauer, C. E. (1994) Directed mutational analysis of bacteriochlorophyll *a* biosynthesis in *Rhodobacter capsulatus*, *J. Mol. Biol. 237*, 622−640.
45. Gibson, L. C. D., and Hunter, C. N. (1994) The bacteriochlorophyll biosynthesis gene, *bchM*, of *Rhodobacter sphaeroides* encodes *S*-adenosyl-*L*-methionine: Mg protoporphyrin IX methyltransferase, *FEBS Lett. 352*, 127−130.
46. Rüdiger, W., Bohm, S., Helfrich, M., Schulz, S., and Schoch, S. (2005) Enzymes of the last steps of chlorophyll biosynthesis: modification of the substrate structure helps to understand the topology of the active centers, *Biochemistry 44*, 10864−10872.
47. Tehrani, A., and Beatty, J. T. (2004) Effects of precise deletions in *Rhodobacter sphaeroides* reaction center genes on steady-state levels of reaction center proteins: a revised model for reaction center assembly, *Photosynth. Res. 79*, 101−108.
48. Koblizek, M., Shih, J. D., Breitbart, S. I., Ratcliffe, E. C., Kolber, Z. S., Hunter, C. N., and Niederman, R. A. (2005) Sequential assembly of photosynthetic units in *Rhodobacter sphaeroides* as revealed by fast repetition rate analysis of variable bacteriochlorophyll *a* fluorescence, *Biochim. Biophys. Acta 1706*, 220−231.
49. Neidle, E. L., and Kaplan, S. (1993) 5-Aminolevulinic acid availability and control of spectral complex formation in *hemA* and *hemT* mutants of *Rhodobacter sphaeroides*, *J. Bacteriol. 175*, 2304−2313.
50. Chen, L. X., Wang, Z. Y., Hartwich, G., Katheder, I., Scheer, H., Scherz, A., Montano, P. A., and Norris, J. R. (1995) An X-ray absorption study of chemically modified bacterial photosynthetic reaction centers, *Chem. Phys. Lett. 234*, 437−444.
51. Kobayashi, M., Takaya, A., Kanai, N., Ota, Y., Saito, T., Wang, Z. Y., and Nozawa, T. (2004) Reconstitution and replacement of bacteriochlorophyll *a* molecules in photosynthetic reaction centers, *J. Biochem. 136*, 363−369.
52. Tomi, T., Shibata, Y., Ikeda, Y., Taniguchi, S., Haik, C., Mataga, N., Shimada, K., and Itoh, S. (2007) Energy and electron transfer in the photosynthetic reaction center complex of *Acidiphilium rubrum* containing Zn-bacteriochlorophyll *a* studied by femtosecond up-conversion spectroscopy, *Biochim. Biophys. Acta 1767*, 22−30.
53. Haffa, A. L. M., Lin, S., Katilius, E., Williams, J. C., Taguchi, A. K. W., Allen, J. P., and Woodbury, N. W. (2002) The dependence of the initial electron-transfer rate on driving force in *Rhodobacter sphaeroides* reaction centers, *J. Phys. Chem. B 106*, 7376−7384.
54. Kobayashi, M., Yamamura, M., Akiyama, M., Kise, H., Inoue, K., Hara, M., Wakao, N., Yahara, K., and Watanabe, T. (1998) Acid resistance of Zn-bacteriochlorophyll *a* from an acidophilic bacterium *Acidiphilium rubrum*, *Anal. Sci. 14*, 1149−1152.
55. Bylina, E. J., and Youvan, D. C. (1988) Directed mutations affecting spectroscopic and electron transfer properties of the primary donor in the photosynthetic reaction center, *Proc. Natl. Acad. Sci. U.S.A. 85*, 7226−7230.
56. Scheer, H., and Struck, A. (1993) Bacterial Reaction Centers with Modified Tetrapyrrole Chromophores, in *The Photosynthetic Reaction Center* (Norris, J. R., and Deisenhofer, J., Eds.) pp 165−167, Academic Press, San Diego.

BI701407K